



Published in final edited form as:

Lymphology. 2014 December ; 47(4): 156–163.

CHARACTERIZING AXILLARY WEB SYNDROME: ULTRASONOGRAPHIC EFFICACY

L.A. Koehler, D.W. Hunter, T.C. Haddad, A.H. Blaes, A.T. Hirsch, and P.M. Ludewig

Departments of Physical Medicine/Rehabilitation (LAK, PML), Radiology (DWH), Hematology/Oncology (AHB), Medicine/Cardiology (ATH), Masonic Cancer Center (LAK, AHB), University of Minnesota, Minneapolis, and Department of Oncology (TCH), Mayo Clinic, Rochester, Minnesota

Abstract

The aim of this study was to determine if ultrasound could successfully characterize axillary web syndrome (AWS) and clarify the pathophysiologic basis of AWS as a vascular or lymphatic abnormality, or an abnormal tissue structure. This prospective study evaluated women who developed AWS following breast cancer surgery. Using an 18 MHz ultrasound transducer, images were taken of the AWS cord and compared to mirror images on the contralateral side. A blinded radiologist assessed the ultrasound characteristics of and structural changes in the skin and subcutaneous tissue and formulated an opinion as to the side in which AWS was located. Seventeen subjects participated in the study. No structure or abnormality consistent with AWS could be identified by ultrasound. There were no statistical differences between the ipsilateral and contralateral side in skin thickness; subcutaneous reflector thickness, number or disorganization; or subcutaneous tissue echodensity ($p>0.05$). The radiologist correctly identified the side with AWS in 12 of 17 subjects ($=0.41$). A distinct ultrasonographic structure or abnormality could not be identified in subjects with AWS using 18 MHz ultrasound. The inability to identify a specific structure excludes the possibility that AWS is associated with vein thrombosis or a fascial abnormality, and supports the theory that AWS may be pathology that is not visible with 18 MHz ultrasound, such as microlymphatic stasis or binding of fibrin or other proteins in the interstitial space.

Keywords

axillary web syndrome; cording; Mondor's syndrome; ultrasound; breast cancer; lymphatics

Axillary web syndrome (AWS) is a condition that may occur in the early post-operative period following breast cancer surgery with lymph node removal (1–3). AWS is described as a cord of tissue underlying the skin in the axilla or chest wall that becomes tight with shoulder abduction (Fig. 1) (1–4). There are currently no studies that have successfully shown that medical imaging can demonstrate the nature or origin of the AWS cord. We hypothesized that high frequency ultrasound images of AWS could provide insight into the etiology of AWS and assist with the diagnosis and treatment.

It has been suggested that AWS is a variant of Mondor's disease because AWS has a similar physical presentation (2). Mondor's disease is described as thrombophlebitis of the subcutaneous veins of the chest and presents as a cord on the chest wall, which is painful, tender, and causes skin retraction (2). Mondor's disease ultrasound images are described as showing a tubular structure with no flow, consistent with a thrombosed vein (5,6). AWS and Mondor's disease have a similar clinical presentation and description but no ultrasonographic comparison or correlation has been described. There are differing views on the pathophysiology and etiology of AWS (2,7–9). Some believe AWS is associated with pathology of the lymphatic or venous system or both (2,7–9). Others describe AWS cords as abnormal fascial tissue, but call the tight cord Mondor's disease (9).

High frequency ultrasound has the ability to visualize small superficial structures, such as arteries, veins, and connecting tissue elements in the skin and subcutaneous tissues (10). Reflectors represent a pronounced variation in acoustic impedance across a tissue interface, which is visualized in the subcutaneous tissue as varying length white, hyperechoic lines. Stronger reflectors may appear thicker or whiter. The high protein content of even minimal amounts of lymphedema in the interstitial space would cause areas of coagulation, resulting in thicker, more numerous and more disorganized reflectors in the subcutaneous tissue. This effect can be seen clearly in patients with clinically evident lymphedema. The same process would also be expected to increase the overall echogenicity of the subcutaneous tissue. The aim of this study was to determine the ultrasound characteristics of AWS and clarify the possible pathophysiologic basis of AWS as a vascular or lymphatic abnormality, or an abnormal tissue structure. These findings would then allow a comparison with the imaging characteristics of Mondor's disease.

MATERIAL AND METHODS

The study started with an evaluation of all women aged 18 or older at the University of Minnesota Breast Center who had a diagnosis of early stage breast cancer that was treated with surgery and included removal of one or more axillary lymph nodes. Subjects were eligible if they underwent lumpectomy, mastectomy, or mastectomy plus contralateral prophylactic mastectomy. Subjects with synchronous bilateral breast cancer, previous surgical treatment for breast cancer or any prior surgery in the axilla or shoulder were excluded. The patients who were eventually included in the study were those who developed AWS within 12 weeks following surgery. The principal investigator (PI) assessed for AWS at 2, 4, and 12 weeks following breast surgery. Subjects were identified as having AWS if there was a visible or palpable cord of tissue in the axilla, arm or chest with the shoulder fully passively abducted. The study was approved by the internal review board, and all subjects provided verbal and written consent.

Ultrasound Assessment

Subjects identified with AWS on clinical exam underwent a very carefully modified ultrasound assessment. All ultrasound exams were performed by a single ultrasound technician using a high resolution ultrasound system (Siemens Acuson S2000 with 18L6 HD transducer, Mountain View, CA). The 18 MHz frequency allowed for high definition

superficial imaging that was augmented with a “gel standoff” technique to minimize artifacts caused by tissue compression. The Principal Investigator (PI) (LK) was present for all ultrasounds to accurately mark the AWS cord and position the patient. The AWS cord was marked on the skin using a waterproof marker. Mirror image marks were also made on the contralateral side. Patients were positioned supine with the arm to be examined placed in maximum shoulder abduction. Using the markings as identifiers, the PI placed the plastic cannula from a JELCO (© Smiths Medical) I.V. catheter directly over and parallel to the cord to precisely identify the location of the cord on the ultrasound image.

At the start of each patient’s exam the overall image depth, the time gain/compensation curve and the focal zone were adjusted for optimal visualization of the dermis and subcutaneous tissue. These settings remained unchanged for the remainder of the exam to allow for an accurate comparison of tissue characteristics of the two arms. Transverse images of each cord (i.e., perpendicular to the cord) were taken from just beyond the distal end to just proximal to the central end in increments of the width of the transducer head, which was approximately 1 cm. The JELCO plastic cannula, which was held in position by the PI, was checked prior to each image acquisition to insure that it was correctly marking the exact location of the palpable cord. Two images were taken at each level, one with the JELCO in place and one without the JELCO to eliminate the possibility that the JELCO shadow would obscure the cord. The two images were presented for interpretation side-by-side on a split screen (Fig. 2). An ultrasound video clip of each cord was taken with the transducer again positioned transverse to the cord and moving from distal to proximal along the cord, starting and stopping 1 cm beyond each end of the cord. A JELCO was not used for the video clips. Ultrasound images were always acquired first on the left side followed by the right regardless of the side affected. Each arm was rotated and abducted to the same degree.

Ultrasound variables used for analysis

1. Skin thickness (in millimeters): The thickness between the surface of the epidermis and the dermal/subcutaneous junction.
2. Reflector thickness: The thickness of the linear reflectors in the subcutaneous layer, which was defined as one side having reflectors of greater thickness than the other, or the two sides being equal.
3. Reflector number: The number of linear reflectors in the subcutaneous layer, which was defined as one side having more reflectors than the other, or the two sides being equal.
4. Disorganization of reflectors: The degree of disorganization (i.e., not having smooth, continuous alignment) of the reflectors in the subcutaneous layer, which was defined as one side having more disorganized reflectors than the other, or the two sides being equal.
5. Echodensity: This was a subjective visual assessment of the overall echodensity of the subcutaneous layer, which was defined as one side being hyperechoic compared to the other, or the two sides having equal echodensity.

The radiologist (DH) responsible for the ultrasound interpretation was a study co-investigator with over 30 years of experience. He was blinded to the patient identity and the results of the AWS physical exam. He completed the visual comparison of the two sides according to the above criteria then formulated an opinion as to the side in which AWS was present and why. This decision was compared to the actual side with AWS. The radiologist also determined if a cord-like structure or other structural changes that could be associated with a cord were present. If pathology was detected, descriptive information was documented. Documentation included echogenicity, length, thickness and regularity of any abnormal cord-like structures, as well as any changes induced in the surrounding tissue. The layer of tissue involved and the tissue changes at the ends of the cord were also recorded.

Data Analysis

Measurements of skin thickness were analyzed using a t-test, or sign test if non-normality was present. Subcutaneous tissue reflector thickness, number, and disorganization; and echo density (graded as less than, greater than, or equal to the contralateral side) were analyzed using a sign test. A Kappa test was used to analyze the result of the radiologist's opinion as to the side with AWS compared to the actual side. If a patient had more than one cord, an average of the assessments of all of the cords was used for analysis. NCSS 9 was used for statistical analysis.

RESULTS

Thirty-six patients were eligible for the study and all consented to be evaluated. Seventeen of the 36 were diagnosed with AWS and underwent ultrasound assessment. Twelve (70%) were diagnosed at 2 weeks, three (18%) at 4 weeks, and two (12%) at 12 weeks. The age range of the 17 women was 35–73 years old with a mean and standard deviation of 53.4 ± 10 years. Seven patients underwent a mastectomy, seven a lumpectomy, and three a bilateral mastectomy. Twelve patients had a sentinel node biopsy (SNB) with targeted node removal as needed, and five had an axillary lymph node dissection (ALND). The mean number of lymph nodes removed was 3 in subjects with a SNB and 23 in subjects with an ALND. Five subjects developed a post-operative fluid collection. Ten patients were treated with radiation therapy. The ultrasound was done prior to radiation in seven, and after or during radiotherapy in three. Eight patients were treated with neoadjuvant chemotherapy. The ultrasound was done prior to chemotherapy in two, and after chemotherapy in six.

One subject, who initially presented with AWS in the axilla, returned for a second ultrasound after developing a cord on her trunk. The ultrasounds were assessed independently and then combined for data analysis. Analysis of skin thickness; reflector thickness, number, and disorganization; and echo density are presented in Table 1. Skin thickness data was non-normal and was, therefore, analyzed with a non-parametric sign test. There were no statistical differences between the two sides for any of the ultrasound variables. Fig. 3 shows a representative subject with no identifiable structure underlying the marked AWS cord on either side. The study radiologist correctly identified the AWS side in 12 of 17 subjects ($\kappa = 0.41$ -moderate accuracy) primarily based on findings that suggested early lymphedema rather than a cord.

After data analysis showed that the ultrasound was unable to discern the side with AWS or to find a cord, a repeat, more detailed, unblinded evaluation of the study images from the AWS affected extremities was performed, with comparison to the unaffected extremities as needed, to assess for any, more subtle AWS-associated structure or abnormality. The repeat evaluation still showed no consistent patterns, pathologic changes, or identifiable structures that reliably coincided with the location or extent of the cord. In 15 subjects, the radiologist described visible, primarily focal and in distinct findings in the affected extremity that were not seen in the unaffected extremity. In 10 patients, the finding was in the dermis or dermal/subcutaneous junction region, and in five patients in the subcutaneous layer. The terms used to describe the findings near the dermal layer and dermal/subcutaneous junction included a hyperdense structure (Fig. 2), a complex structure of mixed hypo- and hyper-echogenicity (Fig. 4a), or a complex tissue channel that is echogenic (Fig. 4b). In 2 patients, the more complex superficial lesions were associated with a distinct lump in the skin (Figs. 4a and 4b). The terms used to describe the findings in the subcutaneous layer included a “vein-like” or rounded structure visualized to the side of or near the marker, a fluid (hypodense) or hyperdense tissue structure with a thickening of the subcutaneous layer, and a mixed echogenicity structure possibly representing a small neurovascular bundle coinciding with the marker.

DISCUSSION

Despite detailed qualitative descriptions of a variety of pathologic findings near the dermal-subcutaneous junction in the regions identified as containing the clinically palpable cord, no uniform pattern was observed. Three of the subjects had a unilateral cord but a bilateral mastectomy, which may have complicated analysis of the ultrasound results if the surgery resulted in similar ultrasound patterns on both sides. Even in these 3 patients, however, the cord and the AWS side could not be identified due to the lack of a consistent ultrasonographically pathologic pattern.

The final conclusion of the study is, therefore, that a consistent and reproducible structure was not identifiable in subjects with AWS using an 18 MHz ultrasound probe. Although an AWS cord could not be consistently identified with ultrasound, our findings did allow us to compare our findings with those reported in Mondor’s disease. The lack of positive findings in our study also provides support for an alternative hypothesis regarding the etiology of AWS.

Doppler ultrasound findings in Mondor’s disease are most commonly described as a long tubular, anechoic or minimally echoic structure with a beaded appearance and no flow on color or Doppler studies. This description suggests the presence of a thrombosed vein (5,6). One other study in the breast demonstrated a hypoechoic tubular structure with associated skin thickening consistent with superficial thrombophlebitis (11). This type of structure was not identified on any of the ultrasound images in our study. Therefore, AWS does not represent a thrombosed superficial vein, and it is not equivalent to Mondor’s disease.

A 2009 case series on Mondor’s disease described one patient as having clinical characteristics of AWS with a cord in the arm (9). The authors proposed that the cord was

related to an abnormality of the superficial fascia and provided a complex schematic image of fascia corresponding to the region of AWS (9). High frequency ultrasound has proven to be able to identify and distinguish small vessels and fascia in previous studies (10). In our study, no structure resembling abnormal fascia was identified. Therefore, AWS does not appear to be related to a fascial abnormality.

The inability to identify a consistent pattern or abnormal structure in the area of the cord in patients with AWS using 18 MHz ultrasound may be due to the limitations of the technology. Ultrasound of this frequency does not have the ability to detect very small pathology or superficial lymphatics, nor can it provide information about tissue composition without using more sophisticated analytical programs such as a stiffness measurement. The width of the cords could not be objectively measured with a caliper because the cords were palpable but not visible. The width of the cords as determined by subjective clinical assessment by the PI concluded that most cords were 1 mm or less, thus just at or below the level at which they could be detected by ultrasound, particularly when viewed in the midst of the complex echogenicities of the skin and subcutaneous tissue.

It is also possible that the inability to identify a consistent structure is due to the fact that AWS cords are either lymph vessels, since lymphatics are too small to be visualized by ultrasound, or that they are invisible linear collections of high protein lymphedema fluid that are outside small lymphatics and which contain cross-linked fibrin or other proteins. The location of the non-distinct pathologic structures, which were seen on the second more detailed ultrasound review, may also provide support for the lymphedema/small lymphatic hypothesis since 10/17 subjects had visible pathology near the dermal/subcutaneous junction where the superficial lymphatic vessels are located.

A unifying hypothesis is that the cord may be one or more tiny lymphatic vessels tethered to each other or to surrounding tissue by extravasated and cross-linked fluid proteins. In this case, a structure would not be identified by ultrasound as neither the surrounding proteins nor the lymphatics would be visible.

CONCLUSION

No abnormality or structural alteration could be identified in subjects with AWS using an 18 MHz ultrasound probe. Therefore, typically available, high frequency ultrasound does not appear to be efficacious in diagnosing, identifying or characterizing AWS. However, the negative ultrasonographic findings in this study do allow us to draw some important, clinically relevant conclusions about AWS. This study concluded that AWS and the palpable cords were not associated with superficial vein thrombosis or abnormalities of underlying fascia as in Mondor's disease. This study supports the premise that AWS represents localized lymphedema and abnormal or tethered lymphatic vessels since lymphatic vessels and microscopic lymphedema cannot be seen on ultrasound. Further histopathological studies will be needed to confirm this hypothesis.

Acknowledgments

This research was made possible through the support from the Minnesota Medical Foundation and a Doctoral Dissertation Fellowship from the University of Minnesota Graduate School. The authors would like to thank Stephen Schwabacher for performing all of the ultrasounds for the study and give a very special thanks and expression of deep gratitude to all the brave and generous patients who participated in the study.

References

1. Leidenius M, Leppanen E, Krogerus L, et al. Motion restriction and axillary web syndrome after sentinel node biopsy and axillary clearance in breast cancer. *Am J Surg.* 2003; 185:127–130. [PubMed: 12559441]
2. Moskovitz AH, Anderson BO, Yeung RS, et al. Axillary web syndrome after axillary dissection. *Am J Surg.* 2001; 181:434–439. [PubMed: 11448437]
3. Josenhans E. Physiotherapeutic treatment for axillary cord formation following breast cancer surgery. *Pt_Zeitschrift für Physiotherapeuten.* 2007; 59:868–878.
4. Koehler LA. Axillary web syndrome and lymphedema, a new perspective. *Lymph Link.* 2006; 18:9–10.
5. Yanik B, Conkbayir I, Oner O, et al. Imaging findings in Mondor's disease. *J Clin Ultrasound.* 2003; 31:103–107. [PubMed: 12539252]
6. Shetty MK, Watson AB. Mondor's disease of the breast: Sonographic and mammographic findings. *AJR Am J Roentgenol.* 2001; 177:893–896. [PubMed: 11566698]
7. Leduc O, Sichere M, Moreau A, et al. Axillary web syndrome: Nature and localization. *Lymphology.* 2009; 42:176–181. [PubMed: 20218085]
8. Reedijk M, Boerner S, Ghazarian D, et al. A case of axillary web syndrome with subcutaneous nodules following axillary surgery. *Breast.* 2006; 15:411–413. [PubMed: 16257525]
9. Salmon RJ, Berry M, Hamelin JP. A novel treatment for postoperative Mondor's disease: Manual axial distraction. *Breast J.* 2009; 15:381–384. [PubMed: 19601943]
10. Abu-Hijleh MF, Roshier AL, Al-Shboul Q. The membranous layer of superficial fascia: Evidence for its widespread distribution in the body. *Surg Radiol Anat.* 2006; 28:606–619. [PubMed: 17061033]
11. Becker L, McCurdy LI, Taves DH. Superficial thrombophlebitis of the breast (Mondor's disease). *Can Assoc Radiol J.* 2001; 52:193–195. [PubMed: 11436415]



Fig. 1. A visible cord associated with axillary web syndrome of the left medial upper arm 12 weeks post breast cancer surgery (arrow pointing to the structure).

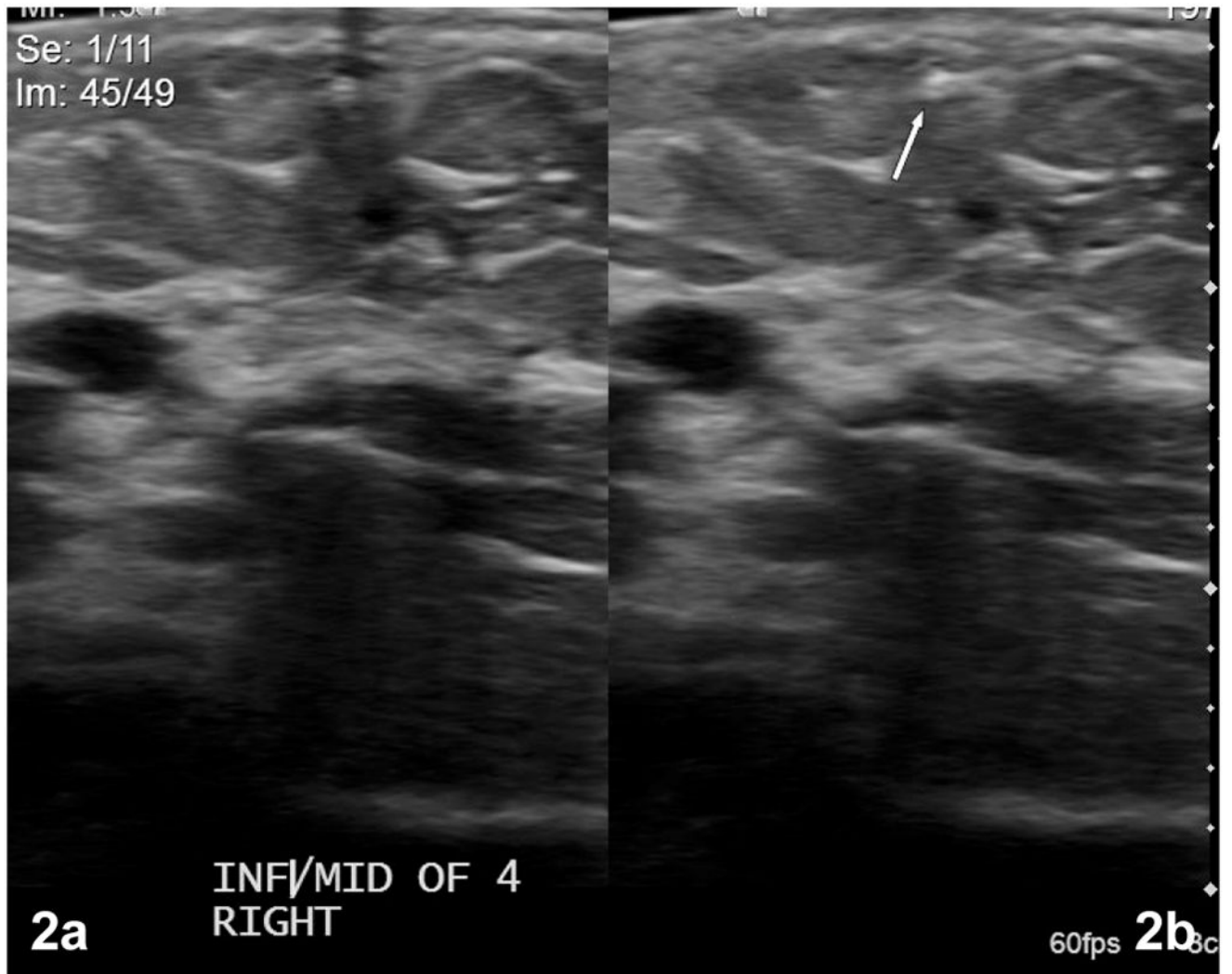


Fig. 2. Ultrasound images of a palpable cord located in the axilla of a 38 year old woman. (a) The white dot near the center of the top of the image is the Jelco on the skin surface, below which shadowing is clearly seen. (b) The arrow indicates a hyperdense structure in the tissue under the marker.

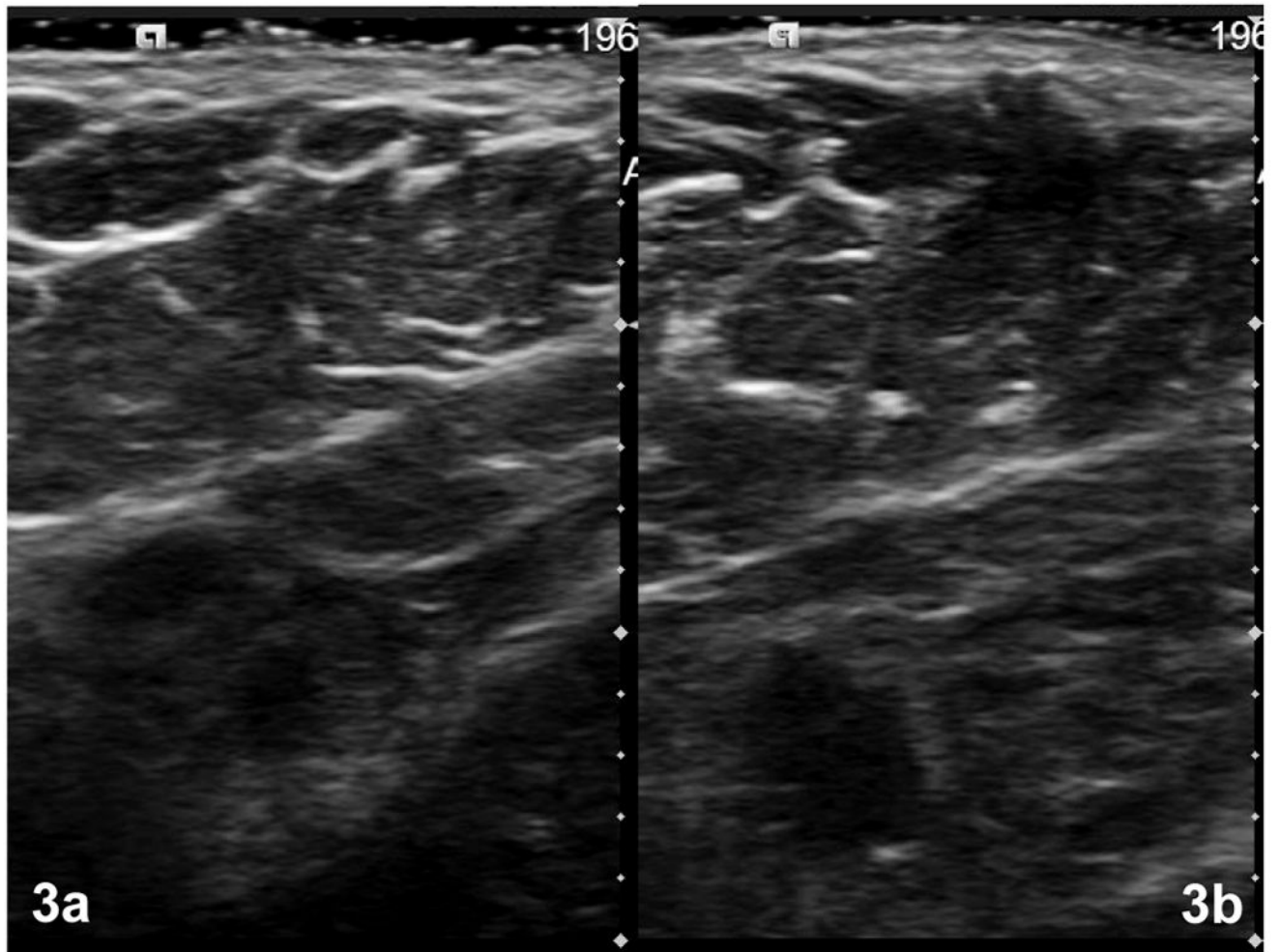


Fig. 3. Ultrasound images of both axillae of a 42 year old woman (without the Jelco marker) showing no identifiable cord-like or other abnormal structures in either the affected side (a) or the unaffected side (b).

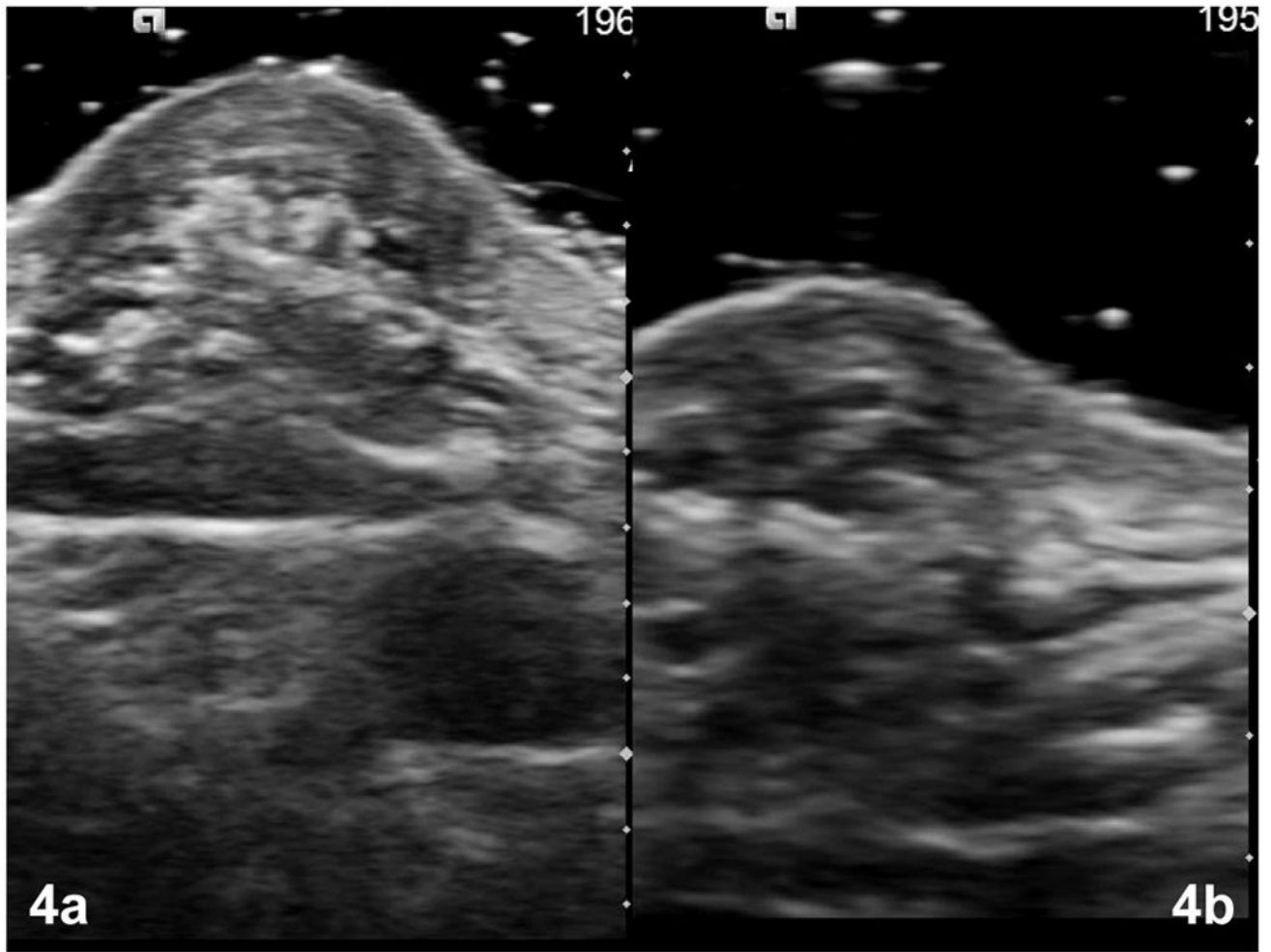


Fig. 4. Ultrasound images of the axillae of the AWS affected extremity in a (a) 42 year-old woman and (b) 52 year- old woman, both of whom had a focal skin lump near the cord on exam.

TABLE 1

Ultrasound Characteristics of Axillary Web Syndrome (AWS) (comparing ipsilateral side to contralateral side)

	Greater than	Equal to	Less than	p-value
Skin thickness	9	3	4	0.27
Reflector thickness	8	7	2	0.11
Number of reflectors	7	9	1	0.07
Disorganization of reflectors	11	1	5	0.21
Echo density	6	8	2	0.29

Author Manuscript

Author Manuscript

Author Manuscript

Author Manuscript